Nanolubricant Oil Additives for Performance Improvement of the Intermediate Gearbox in the AH-64D Helicopter

K.M. Gouda
gouda@email.sc.edu
Graduate Research Assistant
Mechanical Engineering
University of South Carolina
Columbia, SC USA 29208

J.A Tarbutton
jat@sc.edu
Assistant Professor
Mechanical Engineering
University of South Carolina
Columbia, SC USA 29208

Jacob McVay
mcvayja@email.sc.edu
Testing Manager
Condition-Based Maintenance
University of South Carolina
Columbia, SC USA 29208

Abdel Bayoumi
bayoumi@sc.edu
Professor
Mechanical Engineering
University of South Carolina
Columbia, SC USA 20208

ABSTRACT

This paper presents a new nanolubricant for the intermediate gearbox of the Apache aircraft. Historically, the intermediate gearbox has been prone for grease leaking and this natural-occurring fault has negatively impacted the airworthiness of the aircraft. In this study, the incorporation of graphite nanoparticles in mobile aviation gear oil is presented as a nanofluid with excellent thermo-physical properties. Condition-based maintenance practices are demonstrated where four nanoparticle additive oil samples with different concentrations are tested in a full-scale tail rotor drive-train test stand, in addition to, a baseline sample for comparison purposes. Different condition monitoring results suggest the capacity of the nanofluids to have significant gearbox performance benefits when compared to the base oil.

INTRODUCTION

The intermediate gearbox is located on the tail rotor drive-train (TRDT) of the Apache (AH-64) helicopter and it serves the purpose of transmitting torque across the drive-train. The IGB is a grease-lubricated transmission system. The main function of the lubricant is to maintain a fluid film between the moving surfaces, to minimize metal to metal contact in the gearbox when subjected to heavy loads. A secondary objective is to remove heat generated due to friction.

One major problem of these gearboxes is the ejection of grease through their breather port as presented in Figure 1. In the field, this issue presents a serious inconvenience to maintenance crews. Grease leakage can cause the immediate landing of the aircraft to perform extensive maintenance procedures and part removals [1]. After a long period of operation with this fault, excessive wear, erosion, high vibration characteristics, overheating can have a negative impact on the gearbox's performance.

A study was conducted on an IGB at the Condition-Based Maintenance (CBM) test stand at the University of South Carolina. After several hours of operation, an unexpected rapid change of gearbox temperature was observed. An over-temperature of 300˚F occurred and the test stand was warranted for shutdown due to threshold limit exceedance of 295 ˚F. Vibration signatures and tear down analysis findings of the gearbox were inconclusive. There was no indication of abnormal behavior of gear teeth or damage to roller

bearing elements. It was theorized that the reason for this sudden heat generation and grease leaking was not due to mechanical phenomena such as friction and wear, but rather to the chemical decomposition of grease to thin oil.
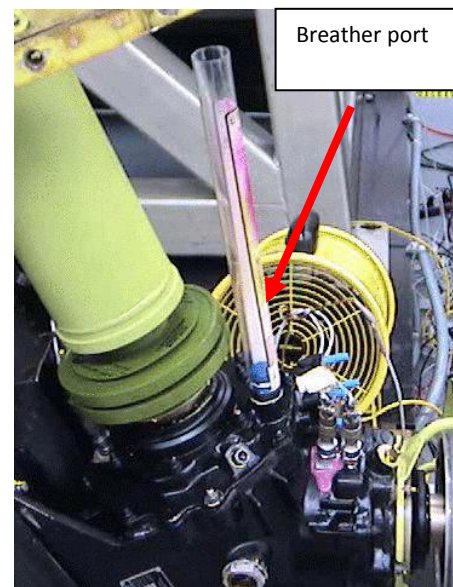

Figure 1. Ejection grease column in intermediate gearbox

Another IGB experiment at USC-CBM [2] was investigated. The main purpose of this experiment was to test the gearbox with oil instead of the conventional used grease lubricant and to compare the performance. Vibration results were inconclusive and, as expected, oil was found to show potential by having a lower operating temperature than grease. A Tail rotor gearbox (TGB) experiment performed by Goodman et al. [3] concluded the possibility of viscosity

---

changes in the lubricant to affect vibration, temperature and some condition indicators (CIs). Consequently, all of these studies have shown one common interest: The need for better lubricant performance in the AH-64 drive-train gearboxes.

Nanofluids have captured huge attention in the past decade as a new class of material with excellent cooling capabilities in a variety of applications [4]. Nanofluids are colloidal suspension of sub-micron or nano-sized solid particles dispersed in the fluid forming a two phase solid-liquid mixture. These nanomaterial additives are dispersed thoroughly in the liquid phase and are intended to boost the thermo-physical properties of the base fluid. Furthermore, the distinctive high surface-area-to volume ratio of the nanoparticles (NPs) enhances surface functionality, resulting in nanofluids having superior heat transfer characteristics when compared to the conventional fluids with no additives.

There are numerous experimental and theoretical studies on nanofluids that have been thoroughly investigated in the literature. For example, Song et al.[5] studied experimentally the rheological properties of different concentrations of nanofluids and nanolubricants using aircraft grease as the base fluid. Another study conducted by Koo et al. [6] was undertaken to understand the mechanism behavior of the NPs and their interactions in the fluid. They theoretically developed a new model to predict the effective thermal conductivity and effective viscosity of nanofluids. The results were in agreement with available experimental data.

Most of the presented literature only suggests the potential of nanofluids in heat transfer applications based on small lab scale experimental investigations or theory. However, the application of nanofluids in complex mechanical systems remains limited and is not sufficiently reported. The main goal of this work is to validate the proof-of-concept of nanofluids and to gain leverage of this new technology for the CBM system. Nanofluids are presented as a new approach for lubrication in a real helicopter gearbox to increase its performance, improve tirbological characteristics and reduce oil temperature which slows breakdown of the fluid film between moving parts.

The purpose of this paper is to study the impact of different nanolubricant additives on the dynamics of the IGB system.

EXPERIMENTAL WORK

Nanolubricant testing

Four samples with different concentrations of graphite nanoparticle additives in the AGL and one baseline oil sample with no NPs were investigated at the CBM test stand. Scanning electron micrographs in Figure 2 revealed the flake like morphology of the particles before dispersion. The particles are expected to be in the range of 100 nm in diameter. Table 1 presents a list of the nanolubricants that were used in testing. In a previous related study [7], these samples were experimentally studied off-line and showed

superior thermo-physical properties than the base oil with no nanoparticles.

Table 1. AGL nanolubricants for testing

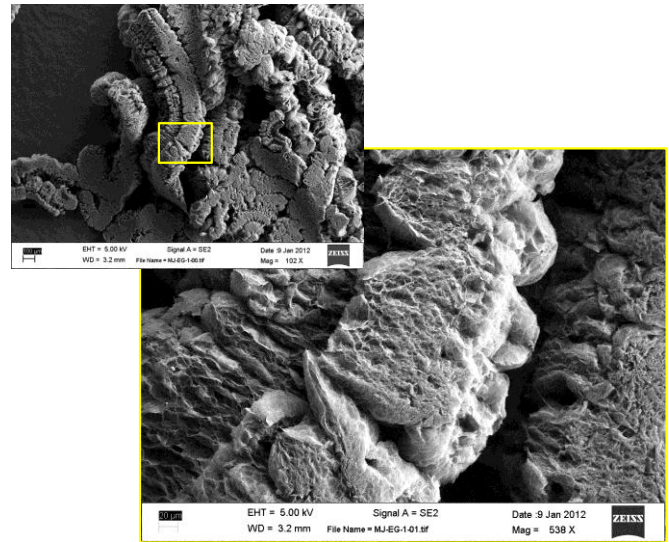| Sample name	Concentration (vol %)	Base Fluid
XG-0A	1 %	AGL
XG-2A	1.5 %	AGL
XG-2B	2 %	AGL
XG-2C	2.5 %	AGL

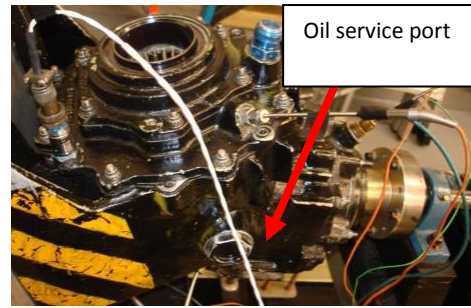**Figure 2. SEM schematics of graphite nanoparticles**

Full-load AH-64 test stand

The CBM test stand at USC is a full-scale AH-64 test stand. It is designed to incorporate all drive-train components and emulate the operating conditions of the drive-train as on an actual helicopter. The test stand is a constant-speed and dynamic-loading power transmission system, starting from the main transmission tail rotor take-off to the tail rotor swashplate assembly. As illustrated in Figure 3, the tail rotor drive shafts are spun at 4863 RPM throughout the duration of a single test run and each test lasts approximately 4 hours. The prime mover for the drive-train is an 800 hp motor controlled by a variable frequency drive. An absorption motor similar to the prime mover creates the braking torque required and acts as a generator. Torque is ramped up from 0 ft-lb to 1223 ft-lb during the experimental run with a 10 minute survey at a constant load step of 111ft-lb. These specific conditions of speed, time of test and load are met to match flight regimes as requested by the Army Engineering Directorate [3]. Overall, the test stand provides a scientific understanding of failure modes of the aircraft drive-train components: Hanger bearings, IGB and TGB.

No-load AH-64 test stand

The purpose of the no-load experiment was to filter out poorly performed samples based on their responses. The no-load test stand in Figure 4 is capable of being used as a preliminary test bed for components before moving to the full-load test stand. Currently, the no-load test stand is set up similarly to the tail rotor drive-train test stand. This test stand is driven by a 5 horsepower motor and it allows for full speed testing of components without applying a torque load. It is to be noted that there are difficulties in establishing which frequencies belong to what components due to noise and/or due to components sharing similar frequencies. For the purpose of this research, as much as possible, analysis is performed as if no other AH-64 vibration information exists.

Figure 3. AH-64 drive-train. Drive-train on actual AH-64 (top) and test stand at USC (bottom)

Methodology

The experimental investigation started at the no-load test stand on an IGB that was removed from an aircraft after completing its required maintenance hours (Figure 4). A design of experiment approach was applied where the five oil samples were tested as the lubricant for the IGB throughout a thirty minute test run per sample. Numerous vibration and temperature responses were monitored and measured via installed sensors. After each experimental run, the gearbox was flushed and drained completely at least 3 times using flushing oil to be ready for the next experiment.

XG-2B was found to be the best performing nanofluid from all the tested lubricants based on the IGB's output characteristics and was moved to the full-load test stand for a 4 hour experimental run where further measurements and

analysis were performed. For comparison purposes, the baseline AGL was also tested for a 4 hour run. Once again,

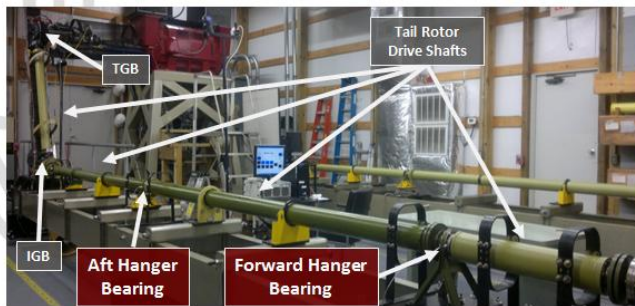several vibration and temperature signatures were measured.

Figure 4. IGB on no-load test stand (Top) and close-up of the IGB used for the testing (bottom)

Data Description

The no-load test stand employs a National Instruments (NI) data acquisition system (DAQ) to collect raw vibration and temperature data. Three acquisitions with a total period of 4 seconds were sampled as shown in Figure 5 during the thirty minute experimental run for the different lubricants.

The full load TRDT employs two DAQs for the collection of vibration, temperature and other data from the drive-train components. The first is known as Modernized Signal Processing Unit (MSPU): a CBM military tool currently installed onboard the AH-64 helicopter (Figure 5). The MSPU is a DAQ optimized for representing processed vibration data, which is the diagnostic parameter or CI. The data is processed through filtering, FFT and other convolution functions built into the MSPU. The second is a NI DAQ that operates in parallel to MSPU and collects the discrete vibration time-series data. A hanning window is used to smooth out responses. NI DAQ runs with custom written code using LABVIEW software and the raw data was acquired simultaneously with MSPU as vibration

surveys during the load steps of the four hour run. These raw vibration data acquisitions were represented as four seconds of total sampling period and both DAQs are survived at a sampling frequency (fs) of 48 KHz. The purpose of the NI DAQ is to help in providing complete information on the health of the gearbox.

Vibration data from both no-load and full-load test sands are thoroughly investigated using temporal, spectral and wavelet analyses.

GEARBOX CONDITION INDICATORS

CIs are an indication of vibration due to mechanical behavior. They are based on the spectral analysis. Multiple CIs are used in the diagnostic process for different components. The following are some of the most common, open-literature algorithms used for machinery diagnostics on gearboxes, specifically for gears[8].

Zero-order Figure of Merit (FM0)

The FM0 is defined as the peak-to-peak of the time signal average normalized by the sum of gear mesh frequency (GMF) and its harmonics:

Figure 5. Vibration data acquisition on the no-load stand (Top) and the MSPU (bottom)

$$FM0 = \frac{\max(x) - \min(x)}{\sum_{i=1}^{n} A(f_i)} \quad (1)$$

where $A(f_i)$ is the sum of amplitudes of the i-th harmonic of the GMF.

FM0 is a robust condition indicator. It is sensitive to major faults in gear meshes such as tooth breakage and uniform wear and an increase in peak- to- peak level is generally observed without significant change in the mesh frequency, which results in an increased level of FM0.

In case of uniform wear, the peak-to-peak does not change appreciably, but the meshing frequencies decrease. The meshing surface is affected and degrades significantly. The energy is redistributed from the GMF to the modulating sidebands and again this result in increase of FM0 values.

Root Mean Square (RMS) of Signal Average

RMS is a good time domain indicator in tracking the overall noise level and is a measure of the power content in the signal. RMS is given by:

$$RMS(x(n)) = \sqrt{\frac{1}{N} \sum_{n=1}^{N} x_n^2} \quad (2)$$

where x_n is the data series of length N.

Fourth-order Figure of Merit (FM4)

This frequency domain indicator is sensitive to localized faults in gear teeth and was developed to detect changes in the vibration pattern resulting from damage on a limited number of gear teeth. FM4 is calculated by applying the fourth normalized statistical moment to the difference signal as follows:

$$FM4 = \frac{-b \pm \sqrt{b^2 - 4ac}}{[\sum_{i=1}^{N} (d_i - d)^{-2}]^2} \quad (3)$$

Where d_i is the difference signal, d is the mean value of difference signal and N is the total number of data points in the time record. A difference signal from a gear in good condition will be primarily Gaussian noise therefore resulting in an FM4 value of 3. As a defect develops in a tooth, peaks will grow in the difference signal that will result in the value to increase beyond 3.

WAVELET ANALYSIS

Wavelet Transform

Wavelet transform is the convolution of the signal x (t) with a set of wavelets of various scales and shifts in time. (Figure 6). The output at a given time and scale is known as the wavelet transform coefficient. The continuous wavelet transform (CWT) is defined in the discrete form as a function of two variables and performs the following inner product operation:

$$C(\tau, s) = \frac{1}{\sqrt{|s|}} \sum_{t=0}^{T-1} x(n) * \psi\left(\frac{(t-\tau)\delta t}{s}\right) \quad (6)$$

Where C is the wavelet coefficient, s is the scale, τ is the translation or the location of the window, ψ is the mother wavelet and the symbol * stands for complex conjugate. The energy of the wavelet is normalized by $1/\sqrt{|s|}$, so that the wavelets would have the same unit energy at every scale.

Mother Wavelet

There are numerous wavelet functions to be used, which are mainly application specific[9]. The wavelet function adopted in this analysis is the Morlet wavelet (Figure 6). The purpose of choosing the Morlet is because of its similarities to the intermittent impulses, which are symptoms of faults in machinery diagnostics. Mathematically, a Morlet wavelet is represented as an exponential decaying cosine function and satisfies both admissibility and regularity conditions.

$$\psi(t) = \exp\left(\frac{-t^2}{2}\right)\cos(5t) \tag{7}$$

Feature extraction using wavelets

Transient characteristics may appear in the form of impulses that instantly die down or appear as high frequency components. Temporal and spectral based CIs can fail to detect these transients due to their inherent limitations of assuming a stationary signal. Transients are produced if the gearbox develops a fault and have to be detected as early as possible. The purpose of applying wavelet analysis in this study is to validate the discrete vibration test stand data with MSPU-CI data of the actual airframe and to extract additional transient information of the gearbox, which is one of the main advantages over the conventional spectral analysis approach.
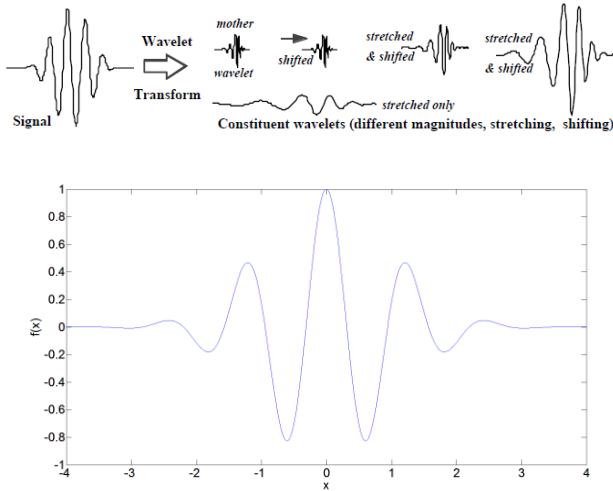
Figure 6. Signal transforming into a number of wavelets of various stretching, shifting and magnitude (Top) and a representation of Morlet wavelet.

The discrete vibration time data is used to determine whether a wavelet approach using the continuous wavelet transforms to detect features is possible Wavelet coefficients are a measure of vibrational energy distribution at a certain scale. These coefficient values can be used as an index to extract the additional attribute for the gearbox. A newly developed wavelet index (WI) is given in equation [8]. The wavelet coefficients from the convolution are first used to compute the wavelet power spectra. Then, the index is computed as a linear combination of the absolute wavelet power spectrum values. In a time-scale plane of a vibration sample, the coefficient values are located at different time shifts and at a particular scale that is expected to cover the frequency band of interests in the gearbox. The WI is then further

normalized by the number of samples for better comparison with other index values.

$$(WI)_S = \frac{1}{N}\sum_{i=0}^{N-1}|C_i(\tau,s)^2| \tag{8}$$

Where $|C_i(\tau,s)^2|$ is the absolute wavelet power spectrum at a given scale s and N is the number of discrete vibration samples.

To relate the wavelets to the actual physical system, the scales can be converted to a pseudo-frequency as follows:

$$F_s = \frac{F_c}{sT_s} \tag{9}$$

Where F_c is the central frequency of the Morlet wavelet, s is the scale and T_s is the sampling period. The equation demonstrates the lower the scale, the higher the frequency and vice-versa.

RESULTS & DISCUSSION

Temperature Response

The operating temperature of the gearbox on both test stands using different lubricants is presented in Figure 7. As expected, the NPs added to the oil lowered the gearbox temperature significantly compared to that of the AGL lubricant with no NPs. During the 30 minute experimental run, the 1.5 and 2% NP samples also known as the XG2A and XG2B, respectively showed an operating temperature of approximately 160° F, which is 40° F less than that of the operating temperature of base AGL. On the other hand, the highest concentration nanofluid of 2% NP; XG2C demonstrated a higher temperature than that of the base oil.
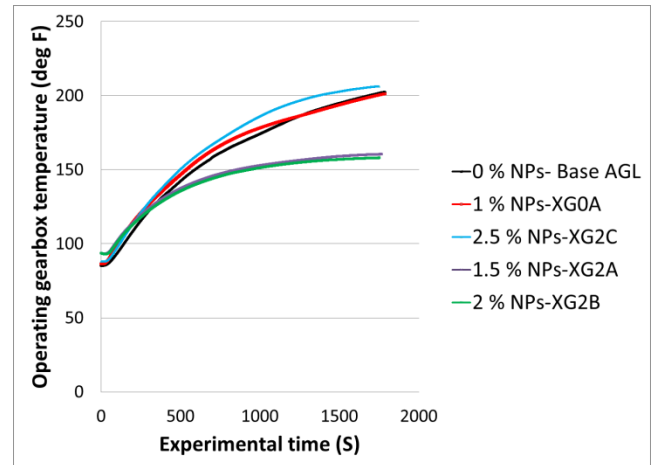
The low operating temperatures of the nanofluids represents their capacity to reduce the breakdown and protect the gearbox from further damage. The addition of NPs to oil absorbs the heat generated due to friction, carries it through the oil and speeds heat transfer between the oil and the metal surface of the gearbox. The heat dissipates away by conduction-convection, resulting in the cooling of the oil.

As for the high viscous oil of XG2C, there was significant amount of foaming observed after testing, which does not make a very good lubricant. This result into an inefficient heat transfer with high operating temperature and more heat generated from the shearing fluid.
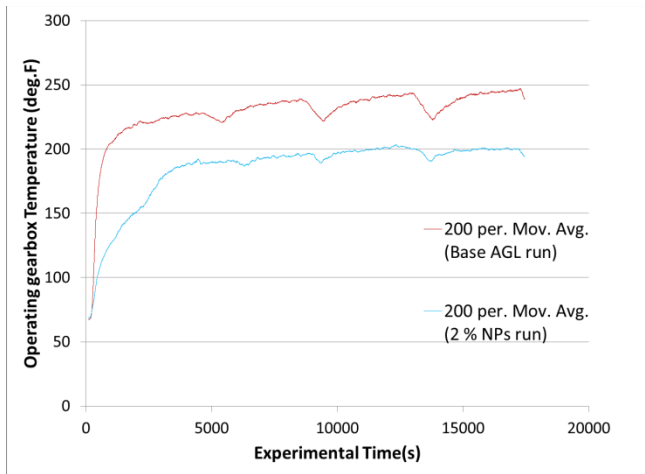

Figure 7. Operating temperature of gearbox No-load (Top) and full-load (bottom)

XG2B temperature profile from the main testing is compared to that of base AGL in Figure 7. This result confirms the no-load testing approach where the nanofluid sample shows an operating temperature of 200˚F, which is 50˚F lower than that of the AGL. It is to be pointed out that the operating temperature at the main test stand is higher due to loading, friction and more heat being generated that emulates the real mechanical system.

Viscosity Response
Effect of shear rate
A rheometer experiment presented in Figure 8 was performed to measure the viscosity at different shear rates. In these measurements, the viscosities at different shear rate values: 1 to 2000 s^{-1} and at a fixed temperature of 40˚C was performed. The experiments were completed five times to ensure repeatability where the average dynamic viscosity value was taken.

All dynamic viscosities of nanofluids prior to testing (fresh) showed a Newtonian behavior (Figure 9). Viscosity data at lower shear rates should be discarded due to experimental uncertainty. The values almost stabilize after a shear rate of 200 s^{-1}. After gearbox testing, the samples were taken for another offline analysis. Results in Figure 9 present the spun oil viscosity as a function of shear rate. The spun NPs had minimum impact on the viscosities of the fluid and presented almost the same Newtonian behavior as that of the fresh samples before testing. However, the high particle concentration of 2.5% NPs; XG2C presented a non-Newtonian or a pseudo shear thickening behavior. This is an indication of more particle interactions, which causes the non-Newtonian behavior and this confirms the high

temperature result presented in Figure 7. It is hypothesized that the NPs for the XG2C were not thoroughly distributed during testing.
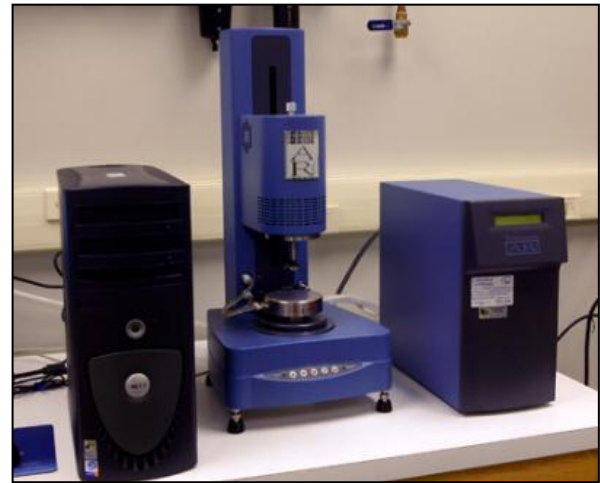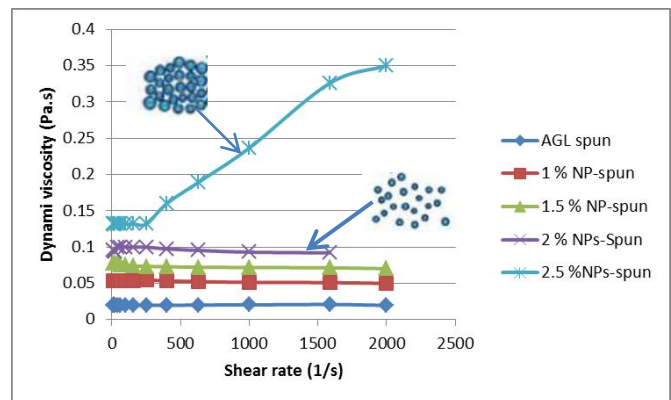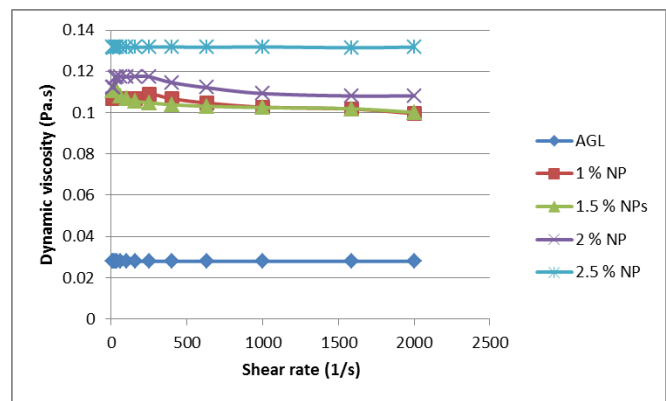

Figure 8. RA-2000 rheometer

Figure 9. No-load results of dynamic viscosity as a function of shear rate Top: Fresh samples as received and bottom: Spun samples after testing

Effect of temperature
The study of temperature dependence on the viscosity of nanofluids was investigated. The main purpose of this study was to determine whether the temperature dependence of

6

viscosity of nanofluids is dominated by the base fluid or influenced by the NPs. The dynamic viscosity of the spun nanofluids was measured with a viscometer at a temperature range of 8-56˚C. For appropriate convenience, a relative viscosity (μ_r) is defined as the ratio of dynamic viscosity of nanofluid to that of the base fluid (μ_{nf} / μ_{bf}).

All relative viscosities of nanofluids in Figure 10 do not change with temperature. However, the μ_r of XG2C showed a slight increase and deviation from the remaining samples.
It may be suggested that the relative viscosity of most the presented nanofluids is independent of temperature and the rheological behavior of nanofluids is mainly dominated by the base fluid itself, even after the addition of the NPs which show to have minimum influence. On the other hand, the increase in the relative viscosity of XG2C with temperature can be due to the NPs, which dominate more than the bulk fluid.

An interesting observed phenomenon observed from this work is that the nanofluid either has Newtonian rheology and temperature independence of the relative viscosity or it has non-Newtonian rheology and temperature dependence of the relative viscosity. However, further investigations are needed to explore this assumption, which goes beyond the scope of this work.
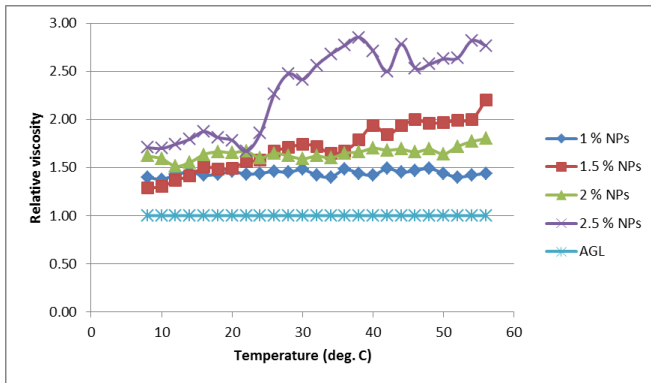

Figure 10. The relative viscosity as a function of temperature for tested nanofluids.

No-load vibration analysis
A time waveform representation of the base AGL sample is presented in Figure 11. Multiple time domain CIs can be extracted from this waveform.

The auto-power-spectrums (PS) of XG2C, AGL and XG2B are summarized in Figure 11, respectively. The PS plots show the majority of energy at the GMF of 3000 HZ with lots of added noise due to the nature of the no-load stand. The cumulative sum of energies from all the experiments is presented in Figure 12 to capture different variations in the PS. The energies start to deviate around the second gear mesh frequency (6000 HZ) and possible higher harmonics with relatively low amplitudes. XG2B has the lowest energy distribution, while XG2C has the highest.
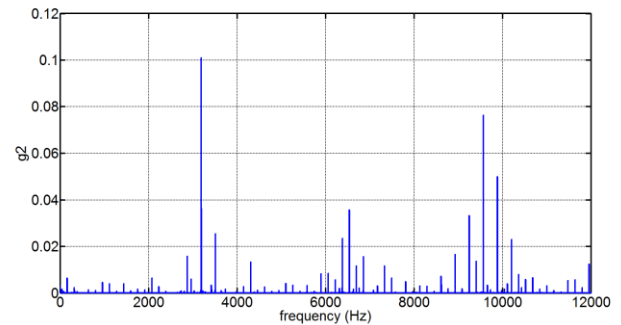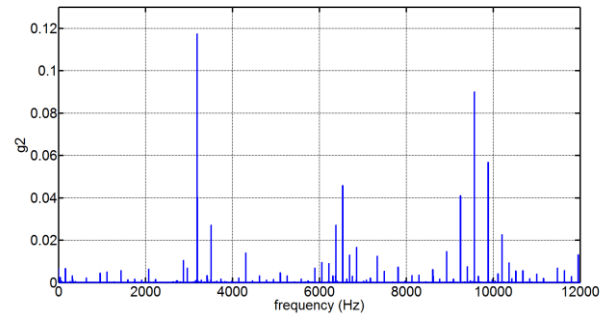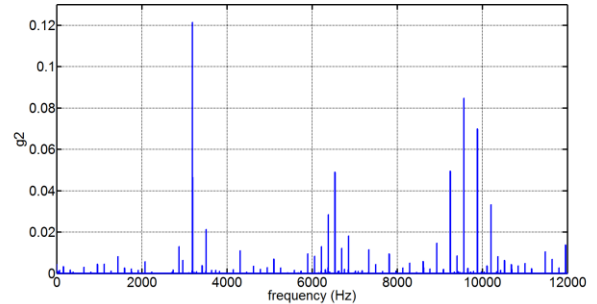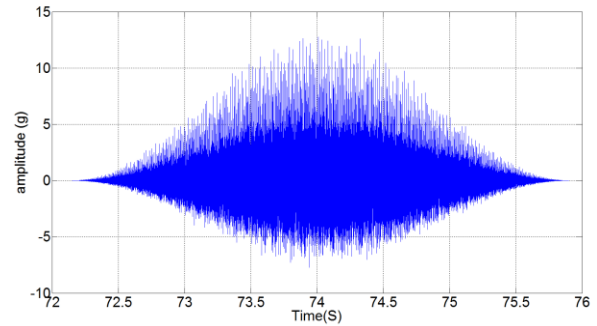

Figure 11. Time-domain waveform and Power Spectrum

CWT scalograms for XG2C, AGL and XG2B are summarized in Figure 13, respectively. To have a complete picture of the scalogram, scales from 1:40 are used in the convolution process. The presented scalograms have some noticeable differences in terms of their wavelet powers. XG2C has highest wavelet coefficients than that of both base AGL and XG2B. Also, XG2B scalogram presents the lowest peaks than the other two. The majority of the wavelet power for all scalograms is located between scales 6-11 (Figure 14)
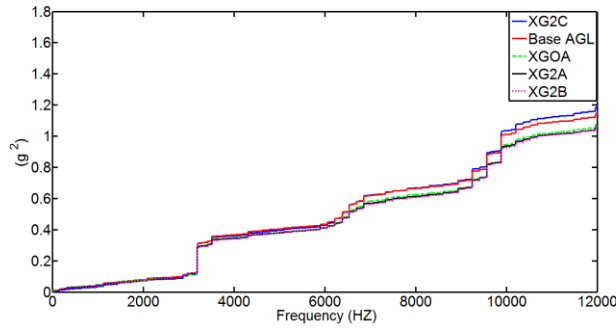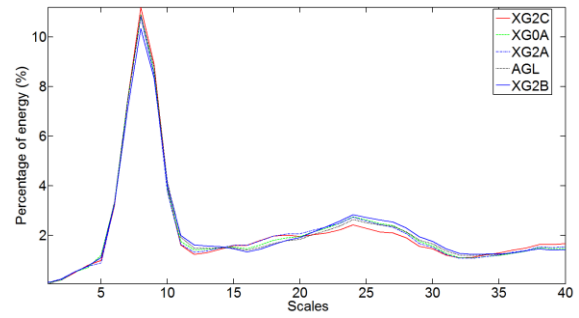
Figure 12. Cumulative sum of energies
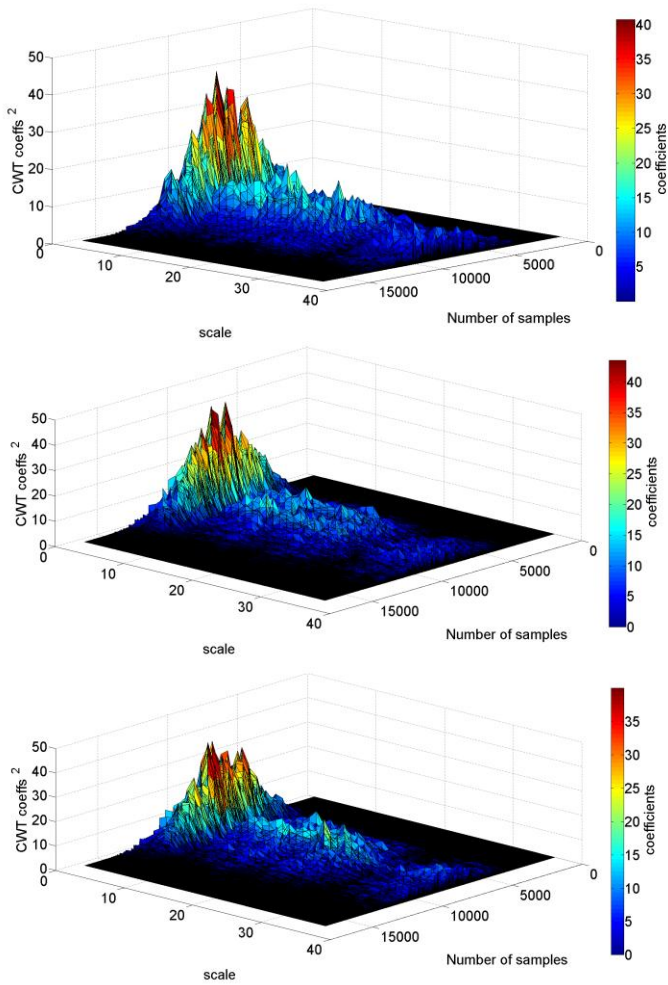

Figure 14. Wavelet power over the scales

Scale 9 corresponds to the GMF, while the remainders of those scales are most likely to be presented as the sidebands. The lower the scale is an indication of higher frequencies and most likely where symptoms or faults start to develop. Consequently, any of the low scales can be used for feature extraction. At this point, it is important to state that a component can have multiple CIs; multiple faults can affect the value of a single CI and a single fault can affect multiple CIs.

Table 2. Scales and the corresponding frequency

S	F_s (Hz)
6	4200
7	4000
8	3250
9	3000
10	2785
11	2437

In this analysis, scale 7 is used for computing the WI from equation [8]. This scale corresponds to a frequency of 4000 Hz and has almost 5% of the wavelet energy. A horizontal slice of the wavelet power (s=7) for XG2C, AGL and XG2B, respectively is summarized in Figure 15. Unlike the Fourier spectrum in Figure 11, the energies at the specified scale or frequency show obvious differences from one experiment to another, which represent the existing transient characteristics. Consequently, WI is extracted and is compared to the conventional CIs of the gearbox.

The proposed WI is compared in Figure 16 with a few vibration-based CIs. FM0 values computed from all no-load oil experiments show little to no change at all with a constant value of 0.05. The RMS values have a trend from high to low; highest value is from the XG2C experiment and lowest is from the XG2B. WCI values are is in agreement with RMS'.

Full-load vibration analysis
The auto-power spectrum from both AGL and XG2B are reported in Figure 17. The data appears significantly meaningful than the spectral analysis of the no-load. Evidently, the gearbox is in a healthy condition and all peaks have low amplitudes where the dominant frequency is the GMF at 3000 HZ, surrounded by a few sidebands and

Figure 13. CWT scalograms

The application of WI is demonstrated using the scalograms. Before feature extraction, it is necessary to choose the scale that can properly represent the system. Furthermore, for an accurate physical interpretation, equation [9] is used to compute corresponding frequencies, which are summarized in Table 2.

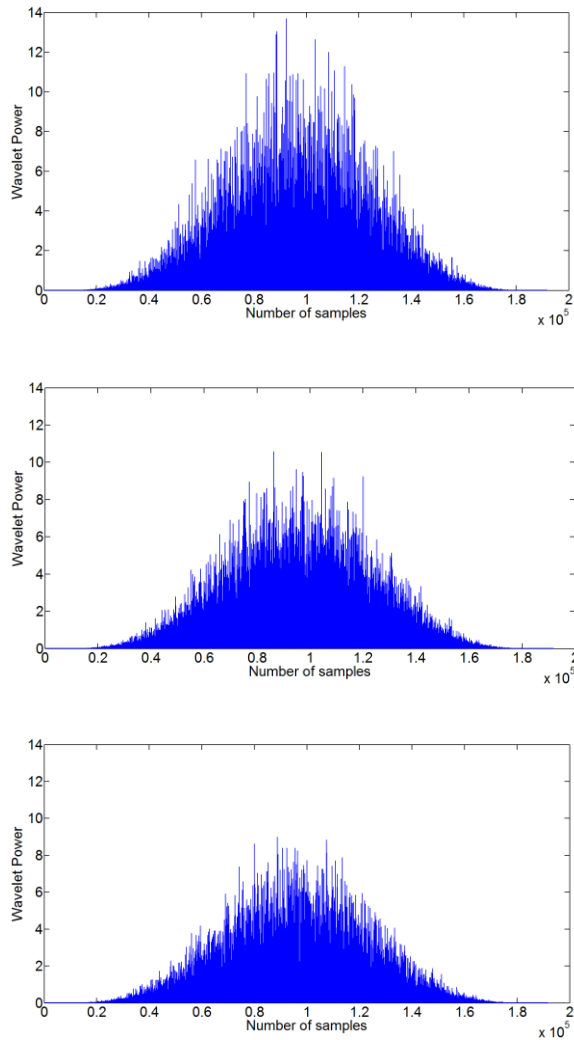bearing frequency of 800-900 HZ.

Figure 15. Horizontal slice of wavelet power at scale 7

Furthermore, the spectrum from the nanolubricant; XG2B has lower energy and sidelobes surrounding the GMF. The cumulative sums of the FFT energies in Figure 18 present a clearer difference, the base AGL appear higher than those from the nanolubricant experiment at higher gear mesh harmonics starting from 2 X GMF.

The CWT scalograms in Figure 19 are displayed after 70 minutes of full-load testing. The convolution process was applied on scales 1:60, which can give redundancy in the transform sometimes. However, the main focus in this work is for feature extraction purposes. There are two regions of wavelet power distributed over the scales. The input and output bearing energy is between scales of 40-60, which correspond to frequencies of 650-1000 Hz. The other region is between scales 9-19, which correspond to the vibrational energies of the GMF and its sidebands. It is clear that there is less wavelet coefficient distribution for the XG2B across both mentioned scale regions. Scale 10 is chosen for wavelet index calculation (f_s=4000HZ), as it represents a considerable amount of the wavelet power.

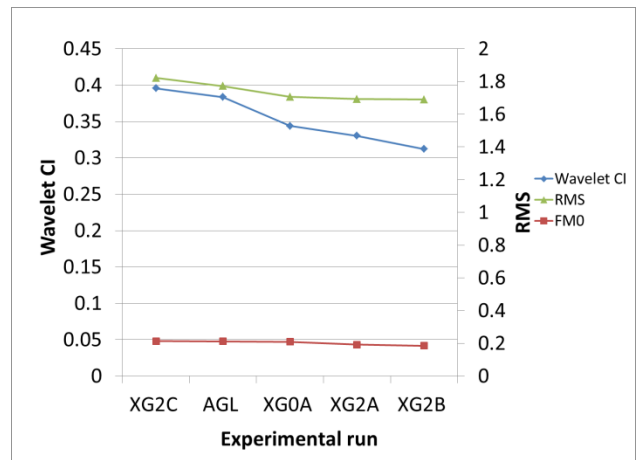**Figure 16. Comparison between different indicators**
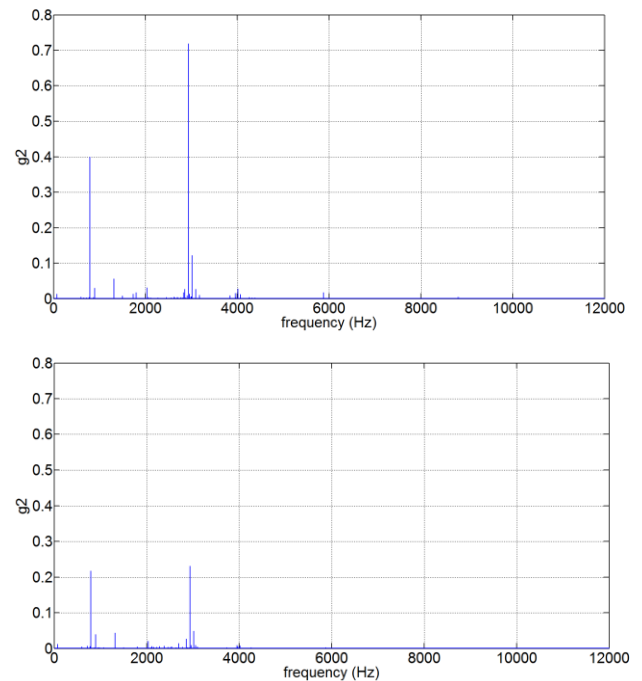

Figure 17. Power spectrum after 130 minutes of testing.
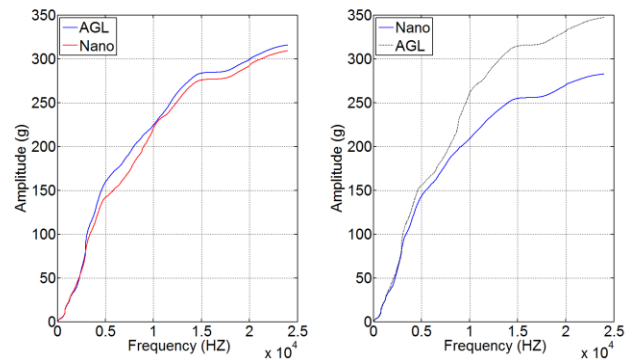

Figure 18. Cumulative sum of FFT energies. Left: after 70 minutes and right: after 130 minutes
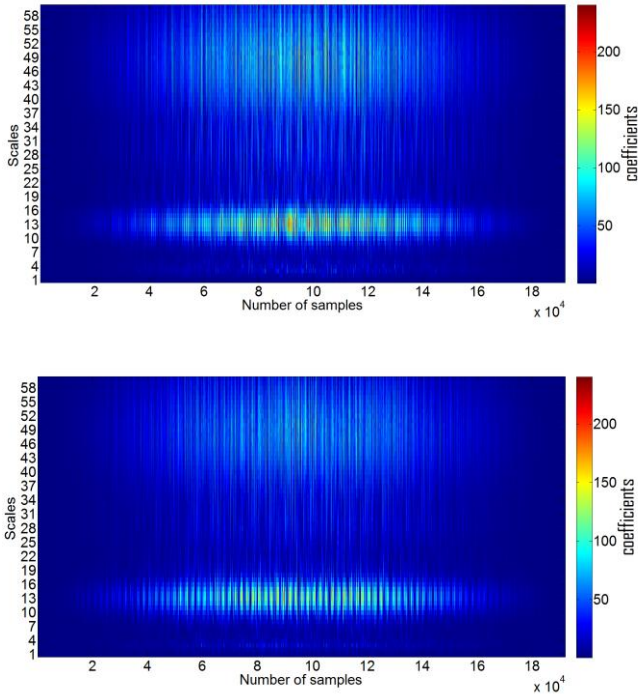
9

Figure 19. CWT scalograms after 70 minutes. AGL (Top) and XG2B (Bottom)

Despite the presence of energy at the high scales (40-60), feature extraction using wavelets would be redundant in this region compared to the conventional spectral analysis. It would make more reasoning to extract a WI near the low scales, which are indicative of possible changes or transients in the collected signal.

MSPU-CIs are compared against each other in Figure 20. The output FM4 CI for the AGL is slightly higher in magnitude than that of theXG2B. This shows the possibility of the NPs to interact with the oil in the gearbox and form a strong film protecting the gears from excessive vibrations. The proposed WI is compared with other existing CIs in Figure 21, which shows the input FM4 and RMS CIs for the AGL higher than those of the XG2B. Furthermore, WCI shows a major difference in trends between both experimental runs in favor of the XG2B with almost a factor of 1.5 in magnitude less than that of AGL. This is because of the ability of wavelets to capture different transient characteristics in the gearbox, which are apparently higher in the case of the base AGL run. These initial vibration results are promising and suggest that the incorporation of NPs in oil has the possibility to protect the surface of the gear during the lubrication regime from possible friction and wear.

CONCLUSIONS & FUTURE WORK

The research efforts in this paper show the promising characteristics of nanofluids to increase the performance of the IGB where different system dynamics have shown

improvement improving the performance of the Intermediate gearbox using nanolubricants. Findings drawn are as follows: (1) Temperature results suggest these nanofluids to significantly outperform traditional oil and to have a positive impact on CBM practices. (2) Incorporation of nanoparticles has evident impact on different dynamics of the system that include: Temperature, vibration and viscosity and the results indicate strong relation among them.
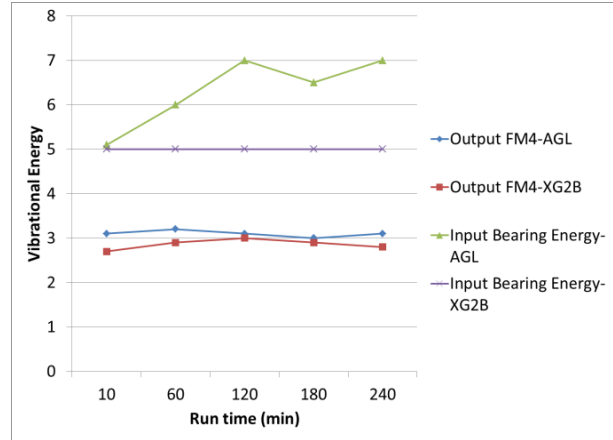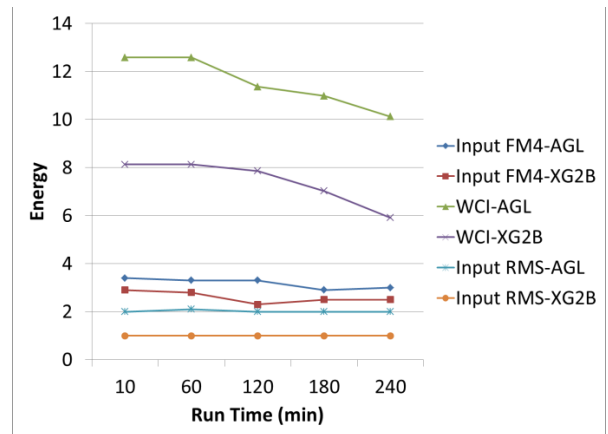

Figure 20. Comparison of MSPU-CIs

Figure 21. WI compared with existing MSPU-CIs

(3) Some conventional condition indicators due to nanoparticle additives have shown a positive impact and a new condition indicator is proposed through the use of wavelets. (4) Low viscous oil nanofluids have better rheology than high viscous oil nanofluids; concentration of nanoparticles above (2%) produces foaming during shearing and this negatively impacts the dynamics of the system. (5) Future testing with rigorous hours is still needed on different gearboxes applying different nanofluid dispersions to further validate the findings proposed and to provide the conclusive assessment necessary to quantify the nanolubrication in a CBM system.

AKNOWLEDGMENTS

REFERENCES

[1] "AH-64 Testing of SHC 626 Oil in IGB-Developmental," RFMR-AED TTS 83442, 2009.

[2] Bayoumi, A., McKenzie, A., Gouda, K., and McVay, J. "Impact of Lubrication Analysis on Improvement of AH-64D Helicopter Component Performance," AHS 68th Conference Proceedings, Fort Worth, TX, May 1-3, 2012.

[3] Goodman, N., Bayoumi, Abdel, Blechertas, V., Shah, R. and Shin, Y.J., "CBM Component Testing at The University of South Carolina: AH-64 Gearbox Grease Studies," AHS 65th Conference Proceedings, grapevine, Texas, May 27-29, 2009.

[4] Saidur, R., Leong, K. Y. and Mohammad H. A, "A review on applications and challenges of nanofluids," *Renewable and Sustainable Energy Reviews*, Vol. 15, (3), 2011, pp. 1646-1668.

[5] Song, B., Yang, Q., Zhang, F. and Su, D. "Rheological Properties of Aircraft Grease Containing Nano-Additives," *Key Engineering Materials*, Vols. 419-420, 2010, pp. 53-56.

[6] Koo, J. and Kleinstreur, C., "A new thermal conductivity of nanofluids," *Journal of Nanoparticle Research*, Vol. 6, 2004, pp. 577-588.

[7] Gouda, K.M., Nikhoo, M., Marcous, S., Bayoumi, A., Tarbutton, J., Eberts, K., Skandan, G., Carr, D. and Eisner, L., "A Study of Nanoparticle Additives on the Performance of the AH-64 Intermediate Gearbox Lubricant to Achieve CBM Objectives," AHS Airworthiness, CBM, and HUMS Specialists' Meeting, Huntsville, AL, Feb. 2013.

[8] Lebold, M., McClintic, K., Campbell, R., Byington, C. and Maynard, K., "Review of vibration analysis methods for gearbox diagnostics and prognostics," The 54th Meeting of the Society for Machinery Failure Prevention Technology, Virginia Beach, VA.

[9] Bendjama, H., Bouhouche, S. and Boucherit, M.S., "Application of wavelet transform for fault diagnosis in rotating machinery," *International Journal of Machine Learning and computing*, Vol. 2, (1), 2012, pp. 82-87.